Wetting behavior of nonpolar nanotubes in simple dipolar liquids for varying nanotube diameter and solute-solvent interactions

Cite as: J. Chem. Phys. **142**, 034704 (2015); https://doi.org/10.1063/1.4905010
Submitted: 09 October 2014 • Accepted: 14 December 2014 • Published Online: 21 January 2015

Malay Kumar Rana and Amalendu Chandra

Wetting behavior of nonpolar nanotubes in simple dipolar liquids for varying nanotube diameter and solute-solvent interactions

Malay Kumar Rana and Amalendu Chandra[a)]
Department of Chemistry, Indian Institute of Technology Kanpur, Kanpur 208016, India

(Received 9 October 2014; accepted 14 December 2014; published online 21 January 2015)

Atomistic simulations of model nonpolar nanotubes in a Stockmayer liquid are carried out for varying nanotube diameter and nanotube-solvent interactions to investigate solvophobic interactions in generic dipolar solvents. We have considered model armchair type single-walled nonpolar nanotubes with increasing radii from (5,5) to (12,12). The interactions between solute and solvent molecules are modeled by the well-known Lennard-Jones and repulsive Weeks-Chandler-Andersen potentials. We have investigated the density profiles and microscopic arrangement of Stockmayer molecules, orientational profiles of their dipole vectors, time dependence of their occupation, and also the translational and rotational motion of solvent molecules in confined environments of the cylindrical nanopores and also in their external peripheral regions. The present results of structural and dynamical properties of Stockmayer molecules inside and near atomistically rough nonpolar surfaces including their wetting and dewetting behavior for varying interactions provide a more generic picture of solvophobic effects experienced by simple dipolar liquids without any specific interactions such as hydrogen bonds. © *2015 AIP Publishing LLC.* [http://dx.doi.org/10.1063/1.4905010]

I. INTRODUCTION

Hydrophobic effects in aqueous media are believed to play important roles in many important physicochemical processes such as folding of protein, micelle-membrane formation, and aggregation of lipids or vesicle formation.[1–5] The high polarity and hydrogen bonding network of water play major roles in determining the solvation structure and dynamics of solutes in aqueous media. At small length scale, a hydrophobic solute can be entrapped by the network of water hydrogen bonds (H-bonds). However, for large hydrophobic surfaces, water molecules cannot extend its tetrahedral H-bonded network and loose significant number of their hydrogen bonds.[6–11] This distinguishes the hydration behavior of small and large nonpolar solutes from the perspective of water hydrogen bonds. Hydration thermodynamics of small nonpolar solutes is entropically controlled whereas that of large hydrophobic solutes is enthalpically controlled.[9,12–16] Due to unfavorable energy loss, water near large hydrophobic surfaces such as those of solutes having diameters more than 1 nm or so[17] is predicted to exist as thin layer of vapor.[16,18,19] The dewetting of large hydrophobic surfaces has also been demonstrated by many theoretical calculations.[14,20–24] The critical length scale of hydrophobic solutes at which hydration thermodynamics changes from entropic to enthalpic regime has been found to depend on various thermodynamic parameters like temperature, pressure, and quantity of the additive substance.[16,25]

Transition of a solute from wet to a dry state has been found to be extremely sensitive to the chemical nature of the hydrophobic unit.[26–28] As an example, we note that despite the extreme narrowness, (5,5) boron nitride nanotube does allow water entrance inside it and produces a wet state whereas (5,5) carbon nanotube (CNT) does not.[29] In addition to the configurational changes, the translational and orientational motion of water molecules also change significantly from bulk properties in the vicinity of the hydrophobic solutes.[30–34] Water in confined hydrophobic nanopores behaves differently than that in the bulk phase. Many of the structural and dynamical properties of water get modified by the geometry of the confining surface. Hydrophobic carbon nanotubes provide an ideal environment where molecular arrangement and dynamics of water can depend strongly on the diameter of the nanotubes.[35–47] These carbon nanotubes, although they are hydrophobic, do not strictly discard water from their nanoscopic pores but control the water structure from single strand to different kinds of shell structures inside them which are held together by hydrogen bonds. Although narrow carbon nanotubes[35] reduce the average number of hydrogen bonds of the confined water, it enhances the population of strongly hydrogen bonded water molecules inside it. Because of this, the narrow carbon nanotubes allow pulse-like motion of water through them.[35,48] Nonetheless, the diffusional behavior of water molecules inside nanotubes is still not fully understood. Unlike bulk water, the water molecules are predicted to show subdiffusive behavior inside narrow carbon nanotubes.[49] In some cases, a combination of ballistic and Fickian diffusion arising from the strong correlation of confined water molecules due to hydrogen bonding interactions has also been reported.[50,51]

The hydrogen bonding interactions are considered to play important roles in the observed structural and dynamical properties of water molecules inside the carbon nanotubes. Almost all the existing simulation work on solvation of carbon nanotubes involve explicit water models as the solvent.[35,36,38–45,47,52–58] However, water is a complex solvent with its hydrogen bonded network greatly determining its

a)E-mail: amalen@iitk.ac.in. Tel.: 91 512 2597241. Fax: 91 512 2597436.

structural, thermodynamic, and dynamical behavior and it would be instructive to look at the structural and dynamical behavior of simple polar liquids in nanotubes where there are no hydrogen bonds in the solvent. Clearly, the motivation to look at this aspect comes from hydrophobic interactions where water hydrogen bonds are considered to play key roles. Here, to address some of the generic issues in this context, we have considered simple model Stockmayer liquid containing a wide variety of single-walled nonpolar atomistic nanotubes of varying diameters and varying solute-solvent interactions. We have carried out molecular dynamics (MD) simulations to study the filling and emptying characteristics of the pores and also of the dynamical properties of the solvent in both interior and exterior regions of the narrow pores. Although the current system does not involve water, we will still use the term "hydrophobic" interaction for convenience.

The outline of the rest of the paper is as follows. Section II describes the details of models and molecular dynamics simulations. Section III deals with structural aspects of Stockmayer molecules in the vicinity of nonpolar solutes of varying size. Various dynamical properties of the solvent molecules are discussed in Sec. IV. Finally, our conclusions are briefly summarized in Sec. V.

II. MODELS AND SIMULATION DETAILS

The nanotubes considered here are of (5,5), (6,6), (8,8), (10,10), and (12,12) types with radii equal to 1.19σ, 1.43σ, 1.90σ, 2.39σ, and 2.86σ, respectively (σ = Lennard-Jones (LJ) molecular diameter). These tubes are considered to be of the same length of 4.7σ and consisting of 120, 144, 192, 240, and 288 carbon atoms. Initially, each tube was immersed in a cubic simulation box containing 1372 Stockmayer molecules corresponding to the reduced density 0.7338. The solvent molecules which overlapped with the nanotubes after insertion were removed from the box. In each simulation, the tube was placed at the center of the simulation box such that its axis points toward the z direction of the box as shown in Fig. 1. The pore atoms were kept fixed at their positions during simulations. The interaction between each carbon atom and Stockmayer molecule is treated explicitly by Lennard-Jones

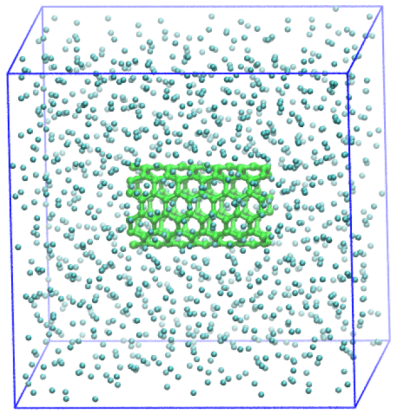

FIG. 1. A picture of the simulation box containing a carbon nanotube immersed in Stockmayer liquid. The nanotube is placed at the center of the box and its axis is parallel to the z axis of the simulation box.

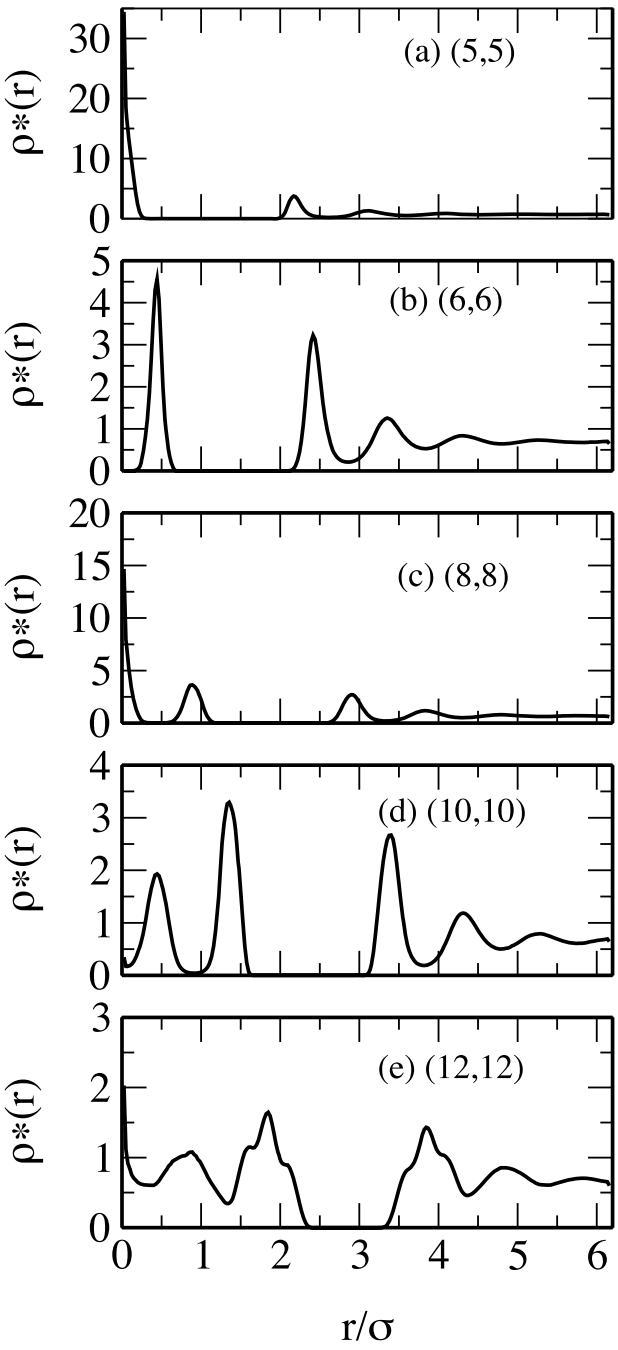

FIG. 2. Reduced density profiles of Stockmayer molecules along the radial direction of (a) (5,5), (b) (6,6), (c) (8,8), (d) (10,10), and (e) (12,12) nanotubes. The results are for systems with solute-solvent interactions described by the LJ potential (called LJ systems).

or by a short-range repulsive potentials as described later. The solvent molecules interact through short-range Lennard-Jones and long-range electrostatic dipole-dipole interactions and the total pair interaction energy between particles i and j can be written as

$$\begin{aligned} u(r_{ij}) &= u_{LJ}(r_{ij}) + Q(r_{ij}) \\ &= 4\epsilon_{LJ}[(\sigma_{ij}/r_{ij})^{12} - (\sigma_{ij}/r_{ij})^{6}] \\ &\quad + \mu_i \cdot \mu_j / r_{ij}^3 - 3(\mu_i \cdot r_{ij})(\mu_j \cdot r_{ij})/r_{ij}^5, \end{aligned} \tag{1}$$

where μ_i and μ_j are the point dipoles located at the centers of the dipolar molecules i and j, respectively. σ_{ij} and ϵ_{LJ} and

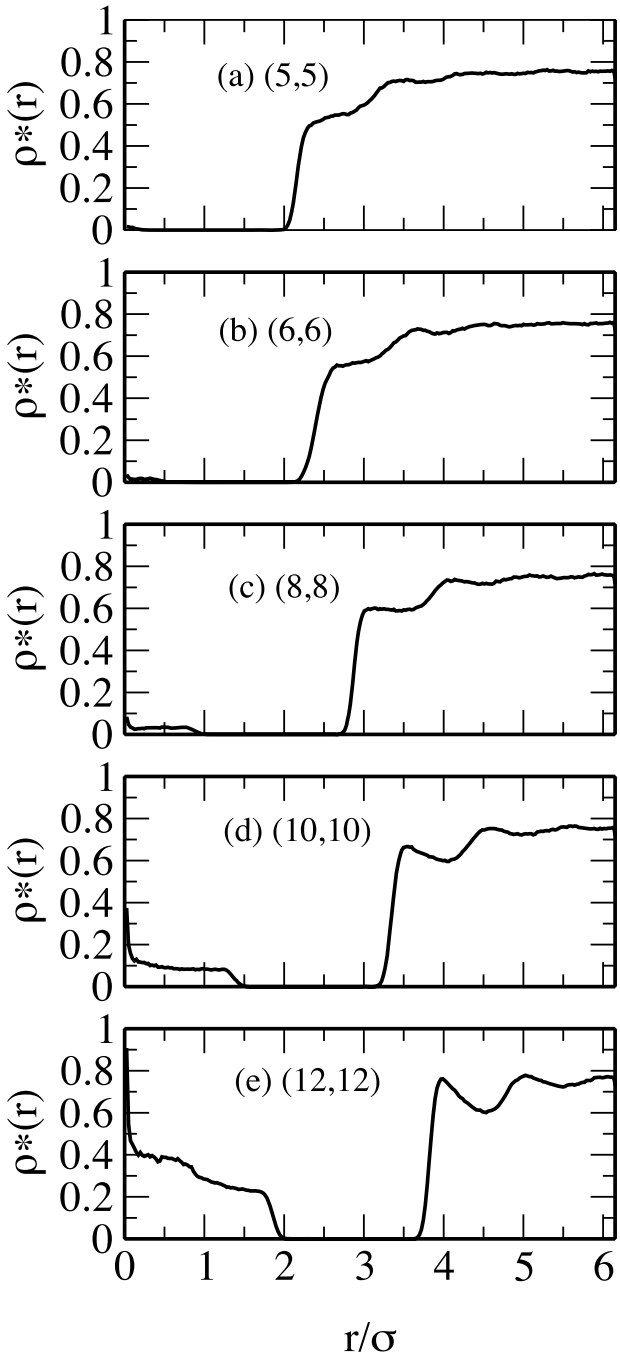

FIG. 3. Reduced density profiles of Stockmayer molecules along the radial direction of (a) (5,5), (b) (6,6), (c) (8,8), (d) (10,10), and (e) (12,12) nanotubes. The results are for systems with solute-solvent interactions described by WCA potential (called WCA systems).

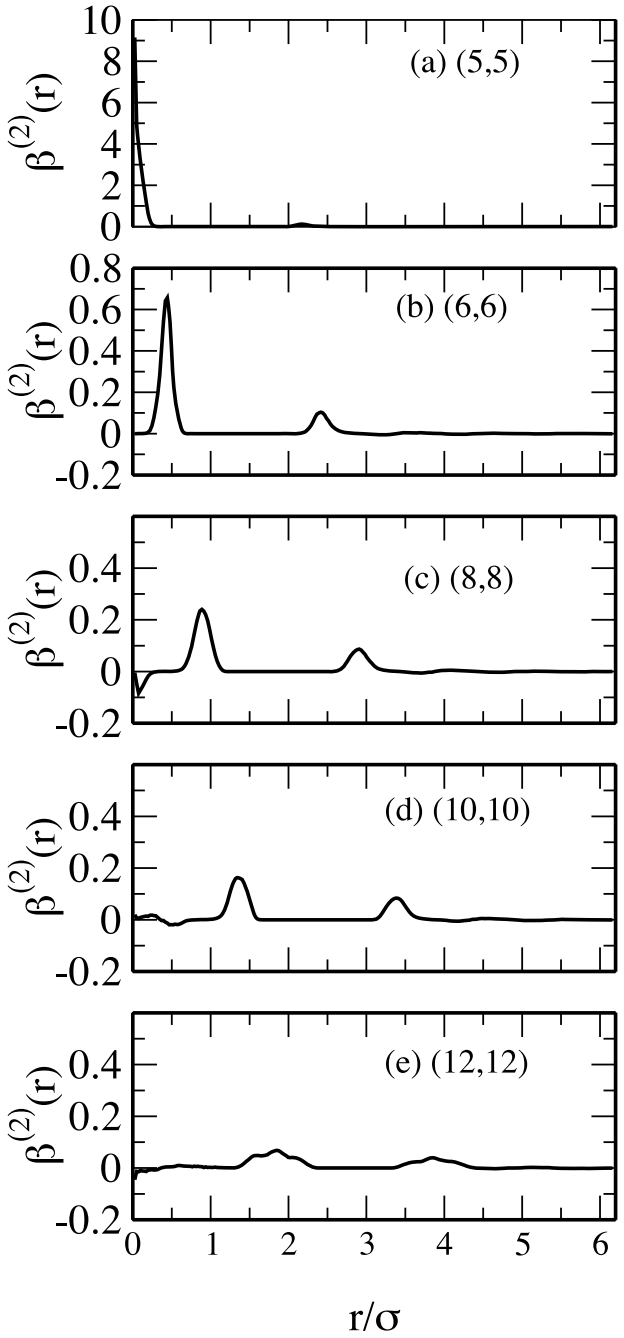

FIG. 4. Second order orientational distribution functions of Stockmayer molecules for five different nanotubes as defined in the caption of Fig. 2.

σ_{ij} are the Lennard-Jones diameter and well depth parameter which are obtained according to Lorentz-Berthelot mixing rules, $\sigma_{ij} = (\sigma_i + \sigma_j)/2$ and $\epsilon_{LJ} = (\epsilon_i \epsilon_j)^{1/2}$. Since the pore (carbon) atoms carry no charge, the nanotube-Stockmayer molecule interaction can be described by the short range term of $U(r_{ij})$. Here, both short-range repulsive and attractive dispersion interactions contribute to the solute-solvent interactions. In the next part of MD simulations, the short range interactions between pore atoms and solvent molecules are treated by the repulsive part of the Lennard-Jones potential as per the decomposition scheme of Weeks-Chandler-Andersen (WCA)[59]

$$u_{WCA}(r_{ij}) = 4\epsilon_{LJ}[(\sigma_{ij}/r_{ij})^{12} - (\sigma_{ij}/r_{ij})^{6}] + \epsilon_{LJ} \quad \text{for} \quad r_{ij} < r_m$$
$$= 0 \qquad \text{for } r_{ij} \geq r_m, \quad (2)$$

where, $r_m = 2^{1/6}\sigma_{ij}$ is the distance at which the minimum of the Lennard-Jones potential occurs. In our simulations, we have assigned the same values of mass and Lennard-Jones parameters to all the species concerned here, i.e., $m_i = m_j = m$, $\sigma_i = \sigma_j = \sigma$, and $\epsilon_i = \epsilon_j = \epsilon$. The reduced dipole moment of Stockmayer molecules is taken to be: $\mu^* = 1.75$. The reduced moment of inertia of solvent molecules is 0.025 and the reduced temperature is kept fixed at $T^* = 1.2$. The reduced parameters are defined as: $I^* = I/m\sigma^2$, $\mu^* = (\mu^2/\epsilon_{LJ}\sigma^3)^{1/2}$, and $T^* = k_BT/\epsilon_{LJ}$, where k_BT is the Boltzmann constant times the

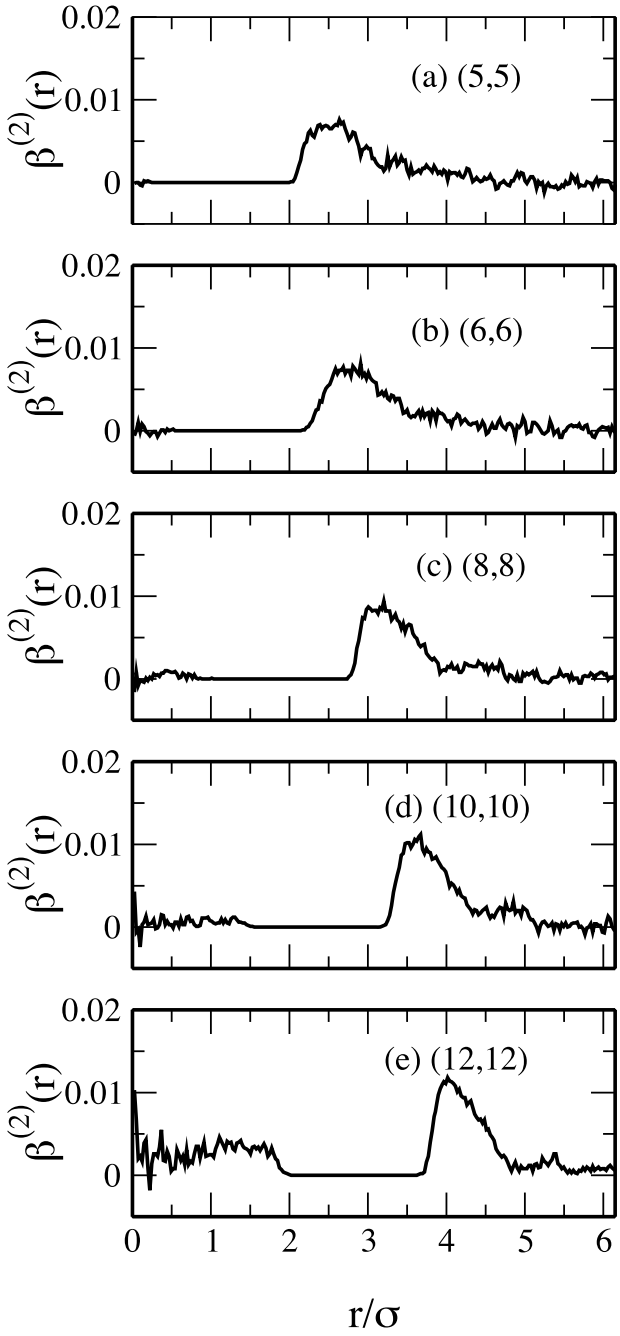

FIG. 5. Second order orientational distribution functions of Stockmayer molecules for five different nanotubes for WCA systems as defined in the caption of Fig. 3.

absolute temperature and the reduced radius is denoted as r^* (=r/σ). It may be noted that the values of various potential parameters of the present systems are chosen so as to keep the systems at a simple level without losing any generic aspects of the interaction of nonpolar solutes with polar solvents. The temperature chosen falls in the range representing the liquid state of the model polar fluid considered here. Although the same values of short range Lennard-Jones potential parameters (ϵ and σ) have been used for the solute-solvent and solvent-solvent interactions in the present work for simplicity, these choices can be easily generalized to consider effects of unequal Lennard-Jones interactions for the solvent-solvent and solute-solvent interactions.

TABLE I. Reduced residence times of Stockmayer molecules in the interior (I) and surface (S) regions of nanotubes. Intermittent residence time is denoted as τ_I^* and continuous residence time is denoted as τ_C^* where $\tau^* = \tau/\sqrt{m\sigma^2/\epsilon_{LJ}}$.

System	Nanotube	τ_I^*(I)	τ_I^*(S)	τ_C^*(I)	τ_C^*(S)	τ^*(B)
LJ system						
1	(5,5)	185.92	19.65	51.92	7.64	∞
2	(6,6)	98.92	21.14	49.48	8.46	
3	(8,8)	135.40	22.36	35.03	10.56	
4	(10,10)	91.58	19.91	30.08	8.56	
5	(12,12)	89.43	20.32	27.24	9.37	
WCA system						
4	(10,10)	4.03	3.02	2.92	0.73	
5	(12,12)	9.35	3.50	4.43	0.87	

We have considered nanotubes of five different pore sizes and, for each nanotube, we have considered two kinds of solute-solvent interactions. Hence, altogether, we have performed simulations of ten different systems. We re-equilibrated the entire system in each case for over 400 000 steps. We used a spherical cut-off at half box length for short-range nonbonded interactions, and three dimensional Ewald method[60] was adopted to account for the long-range electrostatic dipole-dipole interactions. The equations for rotational and translation motions were solved by applying quaternion formulation and leap-frog algorithm with a reduced time step of $\Delta t^* = \Delta t(\epsilon_{LJ}/m\sigma^2)^{1/2} = 0.0025$, and the temperature was maintained through rescaling velocities at $T^* = 1.2$. Thereafter, simulations were continued in microcanonical ensemble for another 1000,000 steps for calculations of various structural and dynamical quantities.

III. STRUCTURE OF STOCKMAYER MOLECULES

A. Density

For aqueous systems, single-walled carbon nanotubes have become the subject of extensive simulation studies where water filling of the carbon nanotubes as narrow as (6,6)[35,42,48,54,55] has been reported. Nanotubes narrower than (6,6) have been found to prevent water permeation, and for tubes with critical diameter and length, liquid-vapor oscillation has been speculated.[61–63] However, with modification of nanotubes[29] or alternatively by changing the strength of attractive dispersion interaction between the carbon and oxygen atoms, filling and emptying features have been found.[35,48] Reducing the attractive dispersion interaction only reduces the water density inside the narrow carbon nanotubes but also in its external peripheral regions. The most vital and interesting aspects of these kinds of nanotube hydration are the diameter dependent microscopic water arrangements in the pore regions[36,42,64] which are attributed to the inter-molecular hydrogen bonding among water molecules and geometric constraint induced by the tubes. Whether the absence of hydrogen bonds in Stockmayer molecules allow similar solvation structure around the uncharged nanotubes is indeed an important issue to be looked at. Therefore, we have calculated the reduced solvent

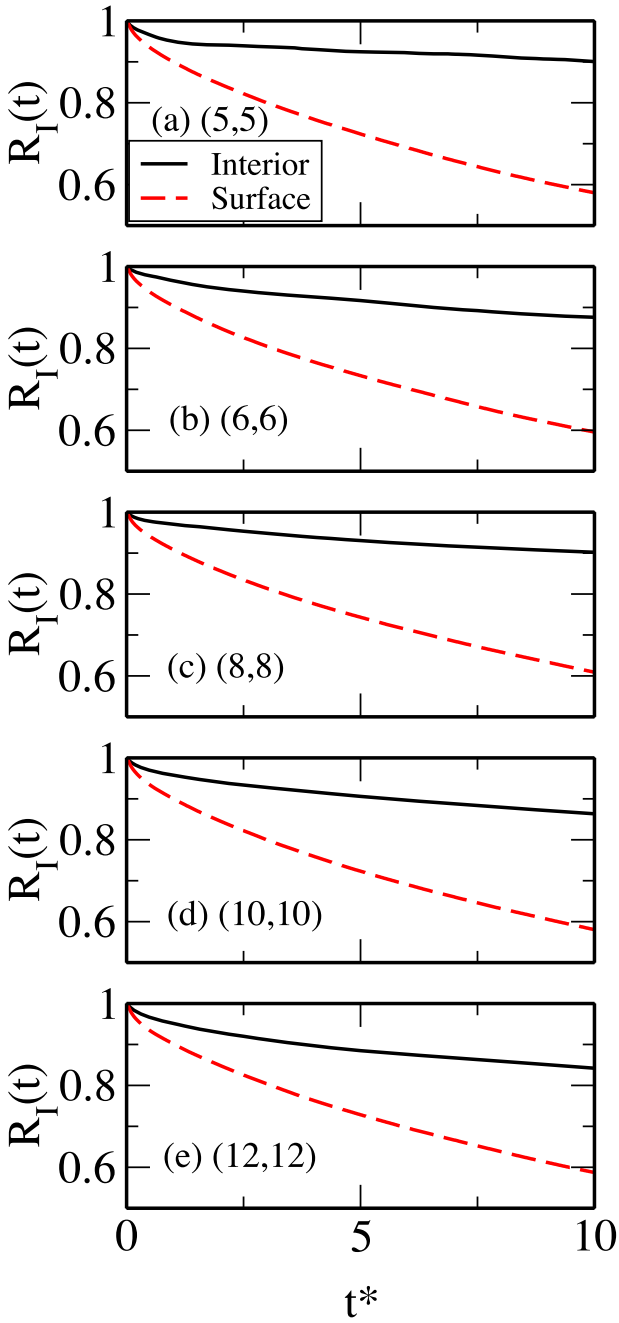

FIG. 6. Time dependence of the intermittent survival probability distribution functions of Stockmayer molecules in the interior (solid lines) and outer wall regions (dashed lines) of nanotubes for LJ systems. The LJ systems are as defined in the caption of Fig. 2.

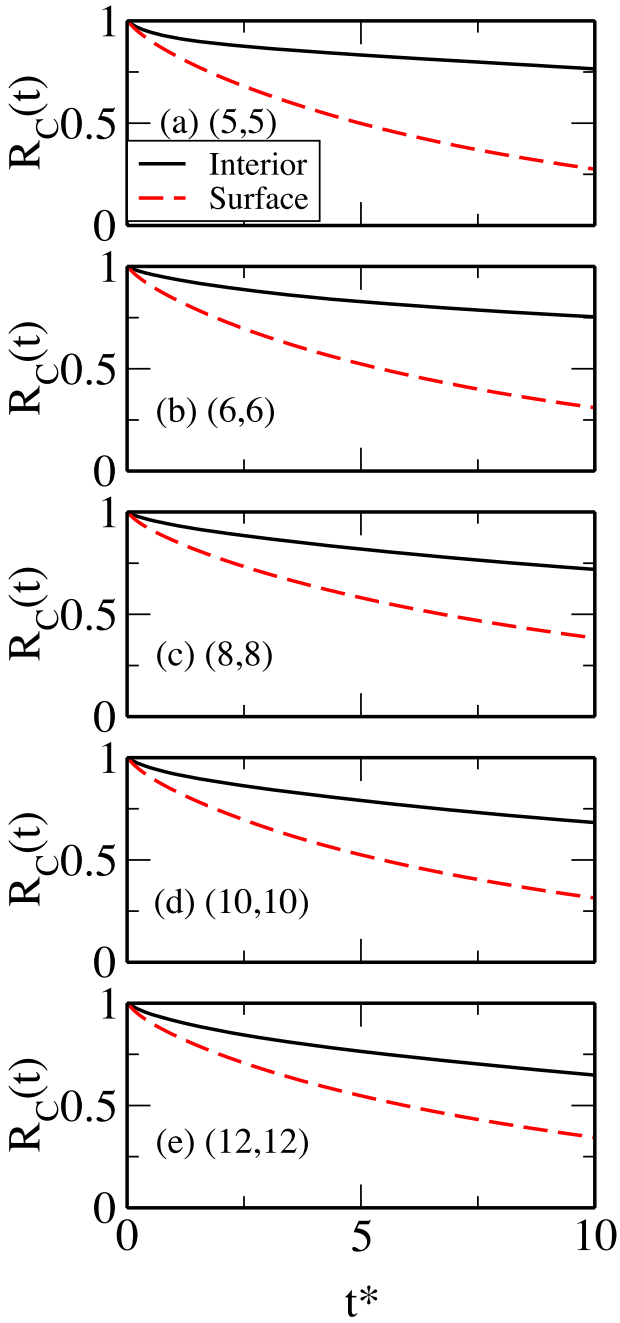

FIG. 7. Time dependence of the continuous survival probability distribution functions of Stockmayer molecules in the interior (solid lines) and outer wall regions (dashed lines) of nanotubes for LJ systems. (See the caption of Fig. 2 for definition of LJ systems.)

density profiles for both types of systems: LJ system where solute-solvent interaction is fully Lennard-Jones type and WCA system where solute-solvent interaction is described by the repulsive WCA interaction. The results of solvent density distributions of these systems are shown in Figs. 2 and 3.

In Fig. 2, we have shown the density profiles for LJ interaction between the Stockmayer solvent molecules and surface atoms. The density profiles have been calculated along the radial direction of the tubes starting from the tube's center set at $r/\sigma = 0$. For this, we have considered many small cylindrical shells of width δr in the xy plane and length equal to the length of the tube. This procedure has been adopted in calculations of all the density profiles and also in subsequent calculation of the orientational profiles of solvent molecules which are presented in Sec. III B. An enhanced solvent density in the interior and also in the vicinity of the external surfaces of the tube is found, which clearly shows filling of the nanotube pores and wetting of the tube surfaces with Stockmayer liquid. The density profiles inside nanotubes of different diameters reveal a one dimensional arrangement of solvent molecules along the tube axis for (5,5), a cylindrical solvent layer in contact with the carbon nanotube surface for (6,6), a cylindrical mono-layer combined with a one dimensional chain at the center for (8,8), cylindrical double-layers of solvent molecules in (10,10), and

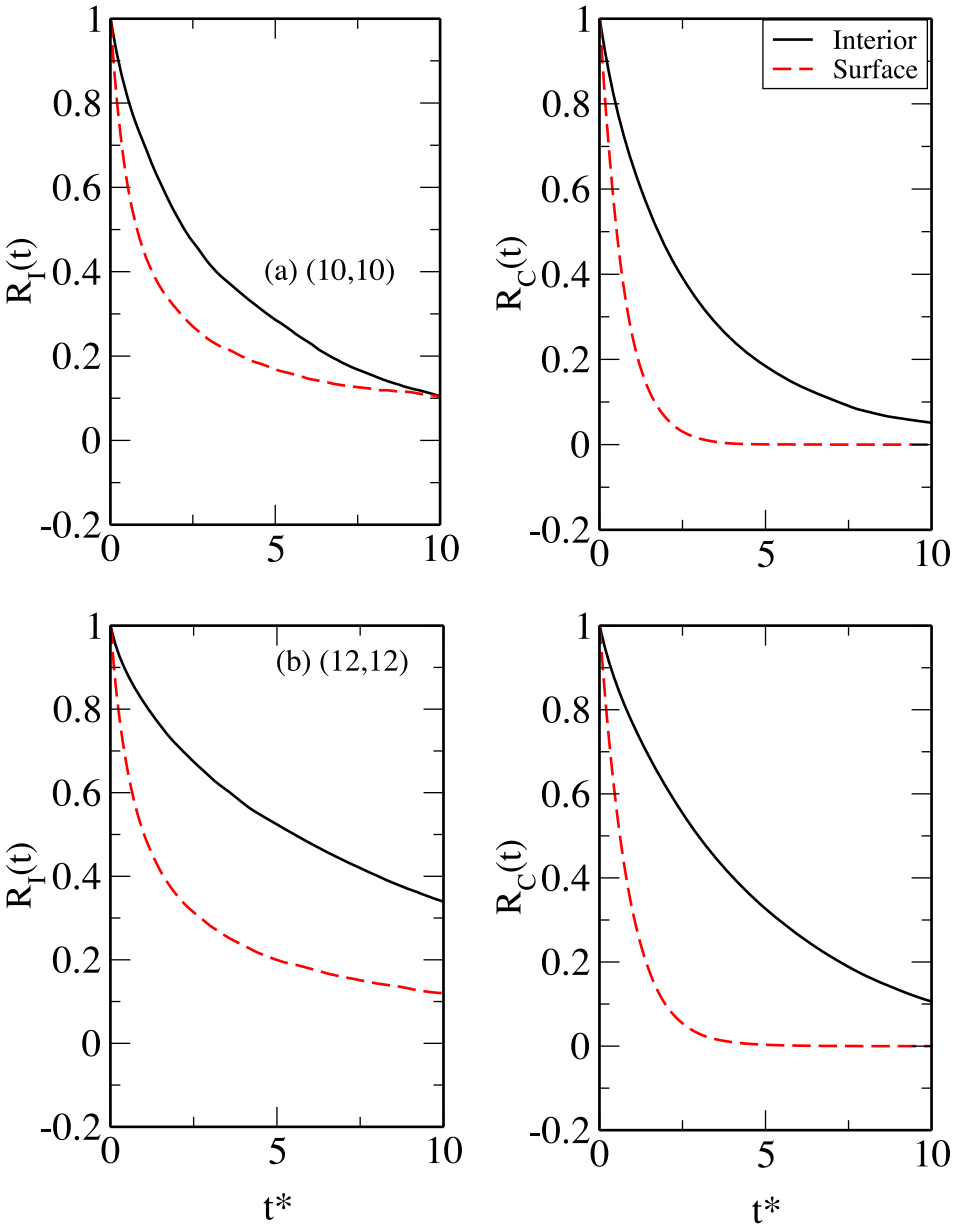

FIG. 8. Time dependence of the intermittent and continuous survival probability distribution functions of Stockmayer molecules in the interior (solid lines) and outer wall regions (dashed lines) of nanotubes for WCA systems: (a) (10,10) and (b) (12,12) CNTs. Left panel is for the intermittent, and right panel is for the continuous probability functions. The WCA systems are as defined in the caption of Fig. 3.

two cylindrical solvent layers containing a chain of solvent molecules along the axis of them for (12,12) nanotubes. The energetic cost associated with the entrance of Stockmayer molecules from bulk region into the tube pore is regained from tube-solvent interactions. In fact, a large number of pore atom-solvent interactions allow the solvent molecules to enter the nanotube or generate a higher solvent density in the proximity of the outer tube surfaces. Here also, the physical volumes of the tubes play an important role in deciding the details of solvation structures. In generic terms, these solvation structures are very similar to those found in the interior regions of water-CNT systems.[35,42] However, a noticeable difference between water and Stockmayer systems arises when we look along the tube axis regions of (5,5), (8,8), and (12,12) nanotubes where probably attractive strength of the surface-solvent interactions and also spherical shape of solvent molecules give rise to more compact arrangement with a higher density for Stockmayer molecules than the density of water molecules in the corresponding water-CNT systems.[42]

For WCA systems, tube walls exert repulsive forces leading to a depletion of the solvent density in immediate vicinity of the external tube surfaces compared to that of the bulk phase. For tubes of relatively larger diameter such as (8,8),

TABLE II. Translational diffusion coefficients in the interior (I), surface (S), and bulk (B) regions. D^*_{xy} and D^*_z are the reduced diffusion coefficients along radial and axial directions. The reduced diffusion coefficient is defined as $D^* = D\sqrt{m/\epsilon_{LJ}\sigma^2}$.

System	Nanotube	D*(I)	D*(S)	D*(B)	D^*_{xy}(I)	D^*_z(I)
LJ system						
1	(5,5)	0.005	0.031	0.11	0.000	0.029
2	(6,6)	0.008	0.033		0.004	0.027
3	(8,8)	0.017	0.032		0.017	0.018
4	(10,10)	0.025	0.032		0.021	0.033
5	(12,12)	0.035	0.031		0.027	0.050
WCA system						
4	(10,10)	0.186	0.132		0.028	0.504
5	(12,12)	0.136	0.121		0.035	0.338

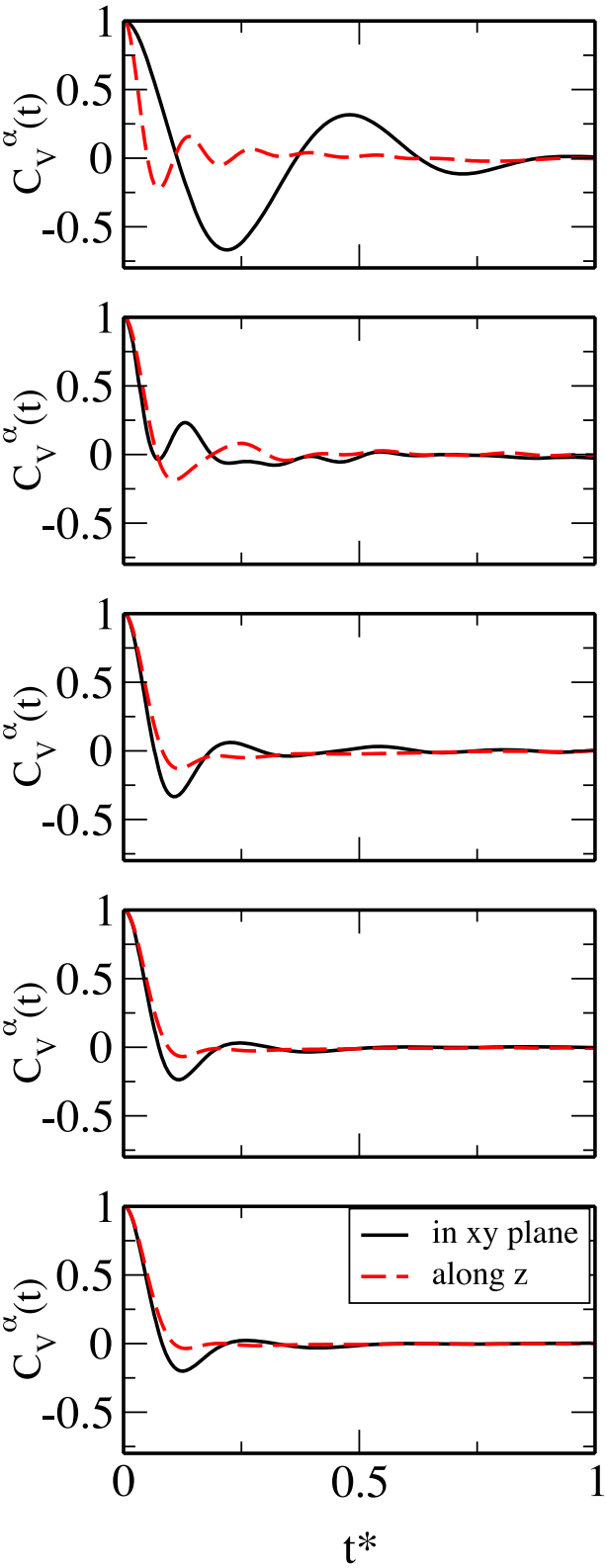

FIG. 9. Time dependence of the normalized velocity autocorrelation functions in the *xy* plane and along the axis of nanotubes for LJ systems. (See the caption of Fig. 2 for definition of LJ systems.)

(10,10), and (12,12) types, weak solvation of the tube pore regions with less solvent density is observed from the density profiles of WCA systems shown Fig. 3. For this repulsive potential, we practically see no wetting of nanopores for (5,5)

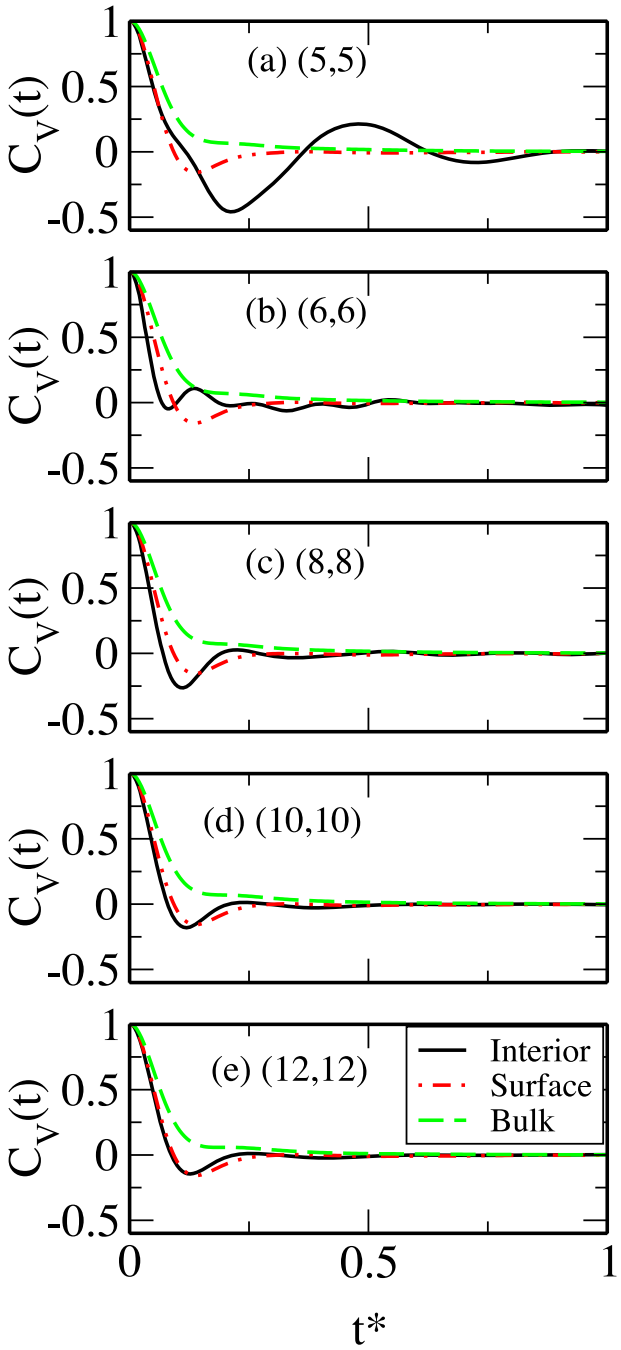

FIG. 10. Time dependence of the normalized velocity autocorrelation functions of solvent molecules in the interior and surface regions of LJ systems and in the bulk. The LJ systems are as defined in the caption of Fig. 2.

and (6,6) types. This repulsive effect also prevents solvent entry of solvent molecules into the narrow tubes.

B. Orientation of Stockmayer molecules

The orientational distributions of dipole vectors of Stockmayer molecules are determined by calculating the position and orientation dependent density $\rho(r,\theta)$, represented as

$$\rho(r,\theta) = \sum_{l} (-1)^{l} \beta^{(l)}(r) P_l(\cos\theta), \tag{3}$$

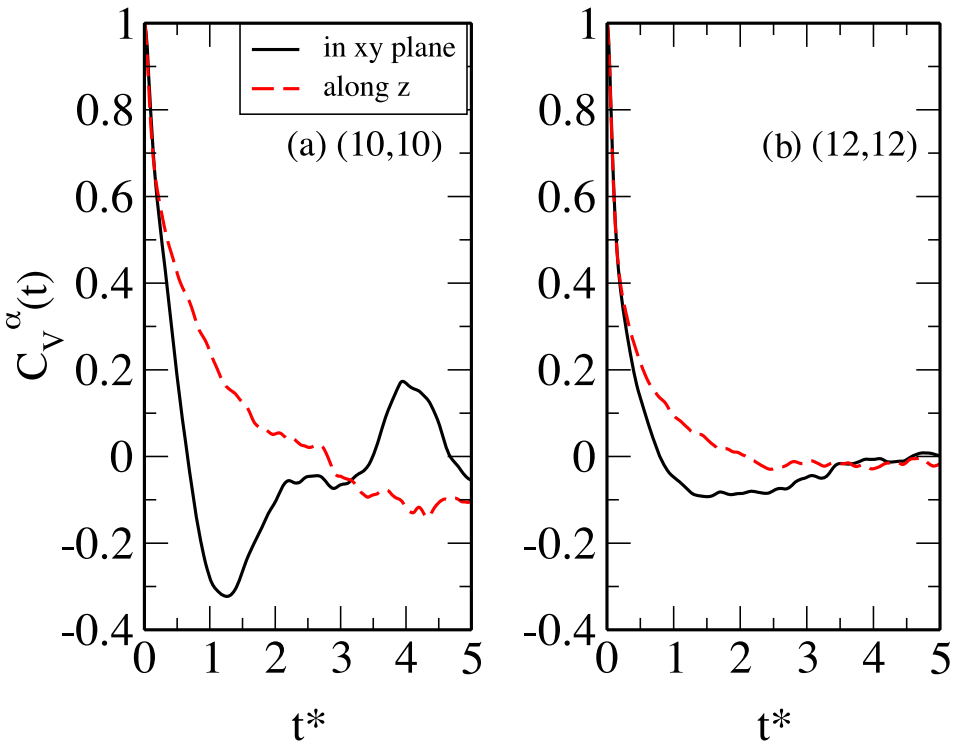

FIG. 11. Time dependence of normalized velocity autocorrelation functions in the xy plane and along the axis of nanotubes for WCA systems. The results are for (a) (10,10) and (b) (12,12) nanotubes. The WCA systems are as defined in the caption of Fig. 3.

where, $P_l(\cos\theta)$ is the Legendre polynomial of order l and θ is the angle between dipole vector of a Stockmayer molecule and the axis of the nanotube, i.e., z-axis of the simulation box. $\beta^{(1)}(r)$ gives information about the arrangement of dipole vectors from tube's center to the bulk. Here, the value of $\beta^{(1)}(r)$ is 0 as the tube surfaces are uncharged and there is no net polarization. Therefore, the most significant term is $\beta^{(2)}(r)$ whose positive value implies that the dipole vectors align along the tube axis and they are parallel to the radius vector of the tube for negative value of $\beta^{(2)}(r)$.

The orientational profiles of Stockmayer molecules for LJ interaction between solvent and surface atoms are shown in Fig. 4. The large positive values of $\beta^{(2)}(r)$ in the narrowest (5,5) tube at the center are a manifestation of very high degree of preference of the Stockmayer molecules to point their dipoles along the tube axis. This alignment is practically absent in wider (8,8) or (12,12) tubes due to the presence of surrounding cylindrical solvent layer/layers where the molecules are involved in electrostatic interactions that rupture the highly ordered dipolar arrangement of single file molecules. Owing to the same reason, the solvent molecules in the innermost cylindrical shell of (10,10) carbon nanotube show no net dipolar ordering. The adsorbed molecules in the inner surface of the tubes show a net ordering perpendicular to the tube radius vector and very small $\beta^{(2)}(r)$ values mean an overall asymmetric distribution. In (8,8), (10,10) and (12,12) tubes, both asymmetric distribution and interactions with innermost molecules are responsible for bringing down the values of $\beta^{(2)}(r)$ for the contact layers. We note in this context that water molecules in narrow hydrophobic channels were also found to possess definite preference to orient their dipoles either up or down the channel axis[65,66] and this trend is interrupted due to appearance of secondary shell of water molecules with increasing radius.[66] For moderate sized channels, small asymmetry in dipole distribution with very small net dipole moments of water molecules has also been reported.[66] For aqueous systems, Won *et al.* found that water molecules in the (6,6) carbon nanotube also point their dipole vectors either toward the top or bottom of the reservoir at any instant.[67] The Stockmayer molecules in contact with the external surfaces of the nanotube also show net dipolar alignment along the tube axis. This orientational trend of dipole moments of Stockmayer molecules seems to corroborate with the results of earlier work[68,69] on water near CNT surfaces. In case of the WCA systems, it is evident from Fig. 5 that the repulsion from solute side prevents any kind of preferential orientation of the dipole vectors of Stockmayer molecules inside nanopore or in the vicinity of the external surfaces. For these systems, $\beta^{(2)}(r) \approx 0$ which is similar to that found for molecules in the bulk region.

IV. DYNAMICS OF STOCKMAYER SOLVENT MOLECULES

A. Residence times

Residence times of Stockmayer molecules can provide useful insight into the dynamical behavior of Stockmayer molecules in the interior and also exterior regions of narrow pores. The solvent residence times are calculated from survival time correlation function approach. We consider the residence dynamics of Stockmayer molecules inside the nanotubes and also near the external surfaces of tubes defined as the first solvation shell immediate to the outer tube-surfaces. These regions are called the interior and surface regions, respectively. We also consider the homogeneous bulk region. The intermittent survival probability function $R_I(t)$ is defined as

$$R_I(t) = \langle \phi_i(0)\phi_i(t)\rangle / \langle \phi_i(0)^2\rangle, \quad (4)$$

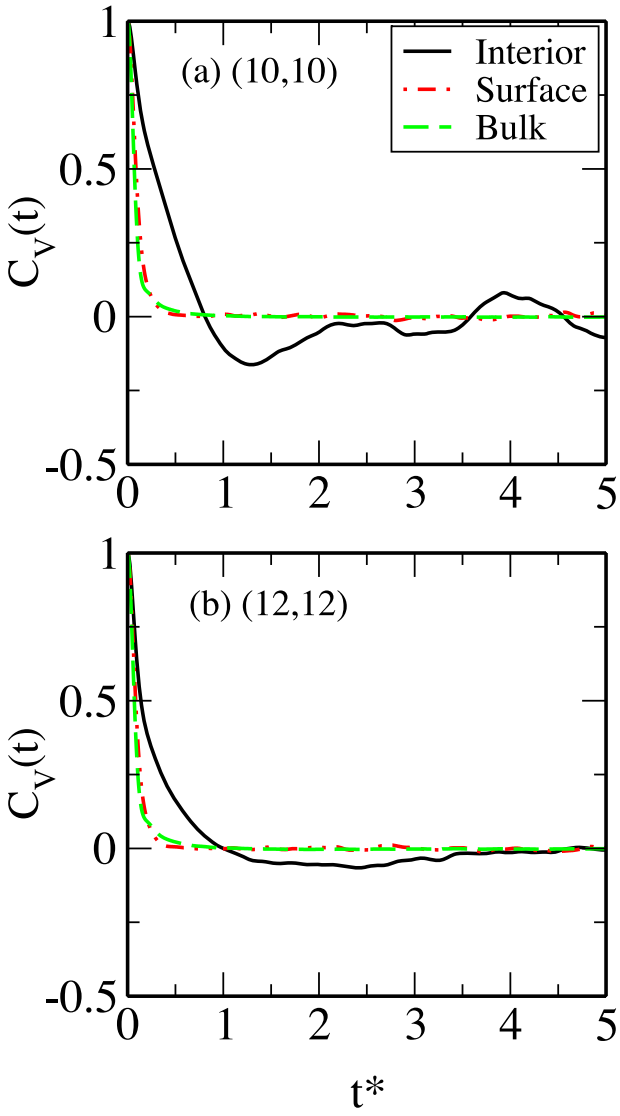

FIG. 12. Time dependence of the average normalized velocity autocorrelation functions of solvent molecules in the interior and surface regions of (a) (10,10) and (b) (12,12) nanotubes for WCA systems and in the bulk.

where $\phi_i(t) = 1$ if the ith solvent molecule is found in a given region at time t, otherwise it is 0. The correlation function $R_I(t)$ describes the probability that a solvent molecule, which was in a given region at time $t = 0$, is also found in the same region at time t. Thus, $R_I(t)$ allows multiple escapes and entries of a solvent molecule in the same region within a given time span. The time dependent continuous probability function $R_C(t)$ is defined as

$$R_C(t) = \langle \phi_i(0)\Phi_i(t)\rangle / \langle \phi_i(0)^2\rangle, \quad (5)$$

where $\Phi_i(t) = 1$ if ith solvent molecule is continuously found in a given region from time $t = 0$ to t, otherwise it is 0. Therefore, the continuous correlation function $R_C(t)$ describes the probability that a solvent molecule, which was in a given region at time $t = 0$, remains continuously in the same region up to time t. Thus, the continuous correlation function does not allow multiple transits of a solvent molecule in the same region during the period from $t = 0$ to t. The average intermittent and continuous residence times, τ_I and τ_C are calculated as integrals of the respective probability functions defined above. The values of τ_I and τ_C are included in Table I for both LJ and WCA systems. The relaxation of the survival probability functions of Stockmayer molecules inside and near the outer wall of nanotubes are shown in Figs. 6 and 7 for Lennard-Jones systems. The functions $R_I(t)$ and $R_C(t)$ for bulk Stockmayer molecules are essentially unity and hence are not shown in these figures. In earlier studies,[70,71] the calculated residence time of water molecules in carbon nanotubes was found to be longer than the corresponding values in the bulk region. Particularly, water molecules inside (8,8),(10,10) and (12,12) carbon nanotubes were found to have longer residence times than bulk water in the order (8,8) > (10,10) > (12,12) > (bulk) at ambient condition.[72] In the present work for LJ systems, the Stockmayer molecules in the interior region of the tubes are found to reside for much longer period compared to that in the surface region (see Table I). Inside the nanotubes, the impacts of wall-solvent interaction and tube dimension alter the residence times and it is seen from Table I that the time constants, both intermittent and continuous, decrease with increase in diameter. It is also observed that the residence times of Stockmayer molecules in the outer surface regions of the tubes are almost equal irrespective of the diameter of the nanotubes.

For WCA systems, the probability functions are shown in Fig. 8. Contrary to the LJ systems, the residence time increases with tube's diameter for surface-solvent repulsive WCA interaction. This can be seen from the residence times of solvent molecules inside the hydrophobic nanopores of (10,10) and (12,12) CNTs (Table I). We have discarded other WCA

TABLE III. Reduced rotational diffusion coefficients (Θ^*) and orientational relaxation times (τ_μ^*) of Stockmayer molecules in the interior (I), surface (S), and bulk (B) regions. $\Theta^* = \Theta(m\sigma^2/\epsilon_{LJ})^{1/2}$ and $\tau_\mu^* = \tau_\mu/\sqrt{m\sigma^2/\epsilon_{LJ}}$.

System	Nanotube	Θ^*(I)	Θ^*(S)	Θ^*(B)	τ_μ^*(I)	τ_μ^*(S)	τ_μ^*(B)
LJ system							
1	(5,5)	0.96	1.94	2.26	65.46	0.33	0.27
2	(6,6)	1.62	2.02		2.40	0.32	
3	(8,8)	1.84	2.03		0.46	0.31	
4	(10,10)	1.93	2.18		0.39	0.26	
5	(12,12)	2.26	2.21		0.29	0.27	
WCA system							
4	(10,10)	17.98	3.03		0.15	0.20	
5	(12,12)	5.02	3.14		0.18	0.20	

systems, i.e., (5,5), (6,6) and (8,8) nanotubes as there are either zero or very few solvent molecules inside these narrower tubes and hence no statistically meaningful results of the residence times could be obtained.

B. Translational dynamics

We have calculated the diffusion coefficients of Stockmayer molecules in the xy plane (D_{xy}) and also along the axial direction (D_z) of the tube pore (D_z) from the respective velocity-velocity autocorrelation functions. The normalized velocity autocorrelation function is calculated as

$$C_v(t) = \frac{\langle v_i(0)v_i(t)\rangle}{\langle v_i(0)^2\rangle}, \tag{6}$$

where the averaging is carried out over those molecules which are found at time instant 0 and at time t with velocity v(t) in the regions of interest. The translational diffusion coefficient is then obtained from the following equation:

$$D = \frac{k_B T}{m}\int_0^\infty C_v(t)\,dt. \tag{7}$$

The values of the translational diffusion coefficient of the Stockmayer molecules are presented in Table II for both LJ and WCA interactions between the solvent molecules and surface atoms.

For each nanotube, it is found that the radial motion of solvent molecules inside the nanotubes is more impeded by the tube walls than the axial motion. This is clearly seen from the velocity autocorrelation functions shown in Fig. 9. The corresponding values of the diffusion coefficients, D_{xy} and D_z, are given in Table II. For these systems, we find a pronounced oscillation and large negative region of the velocity autocorrelation function in interior region of the narrowest carbon nanotube (Fig. 10) which means a significant confinement induced reduction of the rate of translational motion. As the diameter of the tubes increases, solvent molecules inside the tubes move faster. But, in the outer surface regions, the solvent translational dynamics remain more or less the same as evident from the diffusion coefficient values enlisted in Table II. For the larger (12,12) tube, solvent motion inside the tube is comparable with that in the outer region. Overall, confinement and attractive dispersion interaction slows down the translational motion of the model fluid in the interior as well as surface regions compared to bulk. Earlier studies of liquid water inside a series of (n,n) type carbon nanotubes also yielded slower translational motion of confined water molecules compared to bulk water.[39,43,44] In fact, Marti and Gordillo[54] also reported that the axial diffusion coefficients of water are larger than the radial one inside (6,6), (8,8), (10,10), and (12,12) CNTs.[54]

The time dependence of various velocity-velocity autocorrelation functions for WCA systems is shown in Figs. 11 and 12 for (10,10) and (12,12) tubes. Larger diffusion constant values (given in Table II) in tube pore and external wall surface region imply that the wall induced repulsion accelerates translational motion of solvent molecules in and around the tube compared to their LJ analogues.

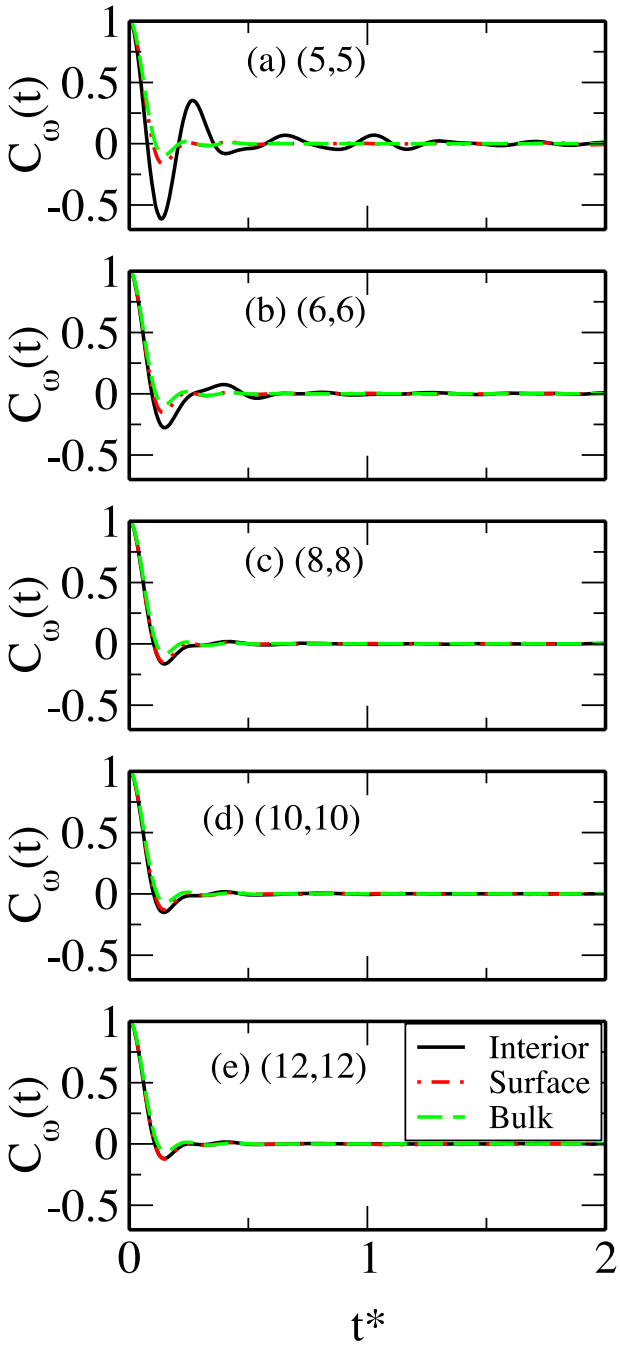

FIG. 13. Time dependence of the normalized angular velocity autocorrelation functions of solvent molecules in the interior, surface, and bulk regions for LJ systems. (See the caption of Fig. 2 for definition of LJ systems.)

C. Rotational dynamics

Rotational motion of Stockmayer molecules can be analyzed by means of the angular velocity autocorrelation function $C_\omega(t)$ and self-dipole moment correlation function $C_\mu(t)$. If $\omega(t)$ is the angular velocity of a solvent molecule at time t, then

$$C_\omega(t) = \frac{\langle \omega(0)\cdot\omega(t)\rangle}{\langle \omega(0)^2\rangle}. \tag{8}$$

The time integral of $C_\omega(t)$ yields rotational diffusion coefficient Θ in the following manner:

$$\Theta = \frac{k_B T}{I} \int_0^\infty dt\, C_\omega(t). \quad (9)$$

Relaxation of the self-dipole vector correlation function with time can be attributed to rotational motion of Stockmayer molecules. Time dependence of the dipole moment correlation function can be obtained from

$$C_\mu(t) = \frac{\langle \mu(0) \cdot \mu(t) \rangle}{\langle \mu(0)^2 \rangle}, \quad (10)$$

where, $\mu(t)$ is the dipole vector of a solvent molecule at time t. The orientational relaxation time τ_μ is calculated from the integral of $C_\mu(t)$. The resulting values of Θ and τ_μ are included in Table III. The decays of $C_\omega(t)$ and $C_\mu(t)$ are shown in Figs. 13 and 14 for LJ interaction between the surface atoms and solvent molecules and in Figs. 15 and 16 for the WCA systems.

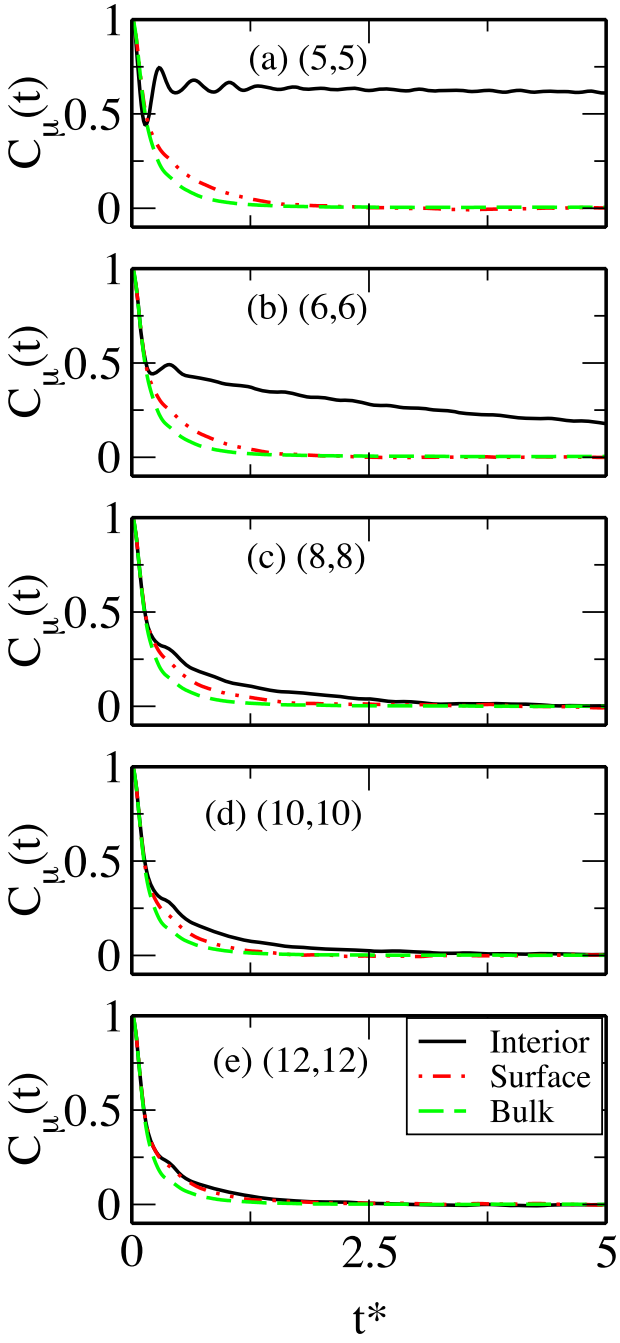

FIG. 14. Time dependence of the normalized self-dipole moment correlation functions of solvent molecules in the interior, surface, and bulk regions for LJ systems.

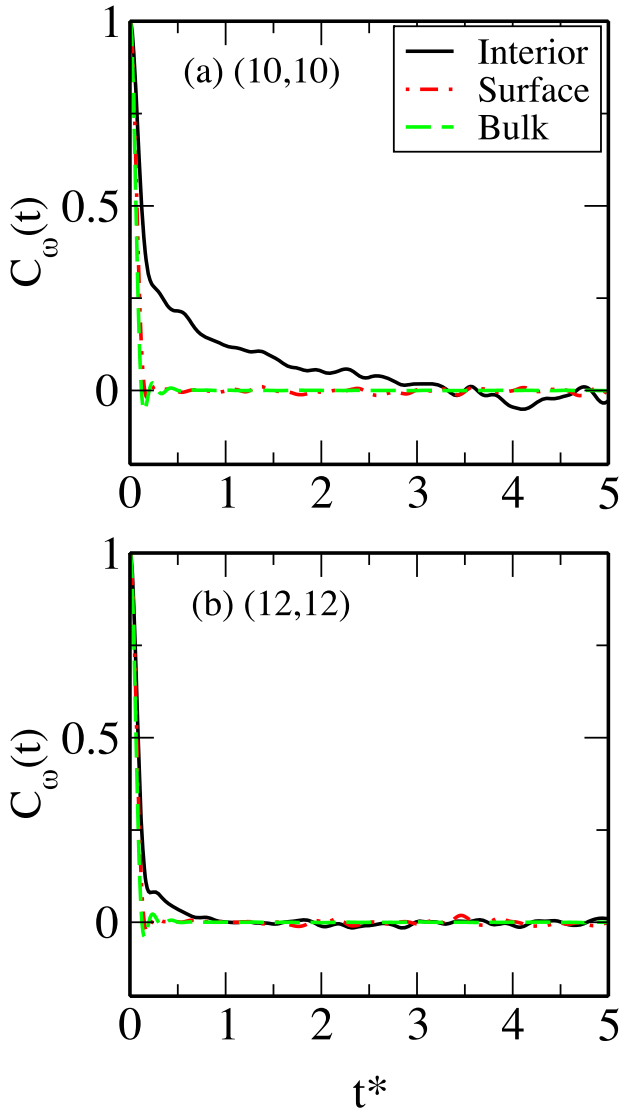

FIG. 15. Time dependence of the normalized angular velocity autocorrelation functions of solvent molecules in the interior, surface, and bulk regions for WCA systems. The results are for (a) (10,10) and (b) (12,12) nanotubes. The WCA systems are as defined in the caption of Fig. 3.

For the systems with LJ interaction between the solvent and solute atoms, smaller values of rotational diffusion coefficients and larger values of dipole moment relaxation times are found for solvent molecules inside the carbon nanotubes which can be attributed to slower rotational motion compared to the solvent molecules in bulk. With increase in tube diameter, rotational motion of solvent molecules in the interior tube regions becomes faster leading to increasing values of Θ and decreasing values of τ_μ from (5,5) to (12,12) tubes. Near the external attractive hydrophobic surfaces, solvent molecules exhibit rotational dynamics comparable with that in the bulk. In the outer tube surface regions, the rotational motion of solvent molecules remains nearly equal as evident from the values of Θ and τ_μ given in Table III. Notably, the values of rotational diffusion coefficients and dipole relaxation times of

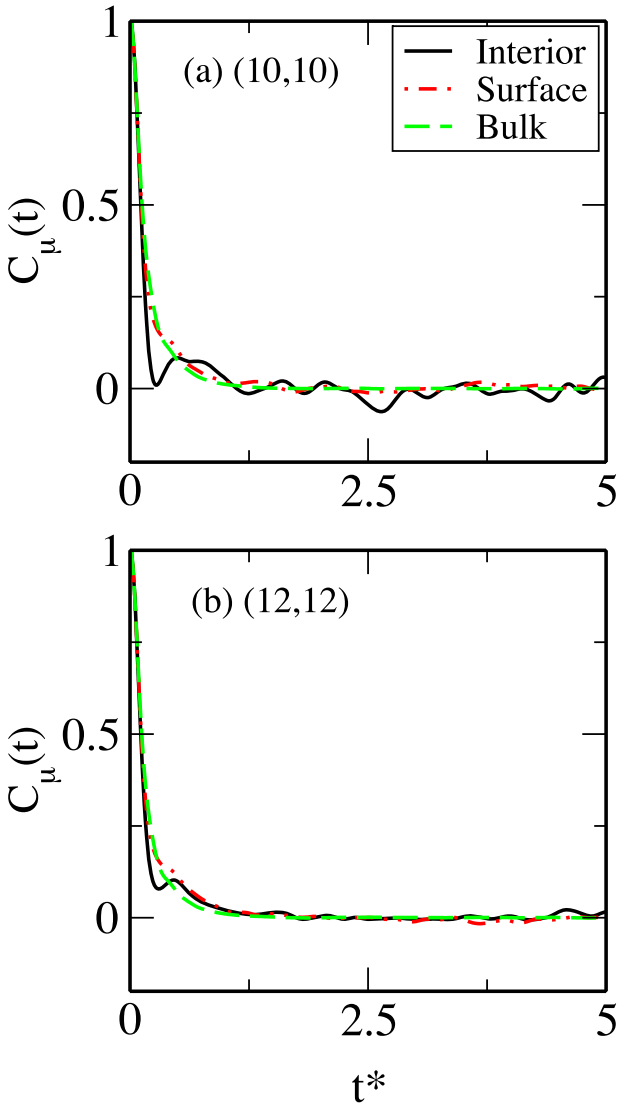

FIG. 16. Time dependence of the normalized self-dipole moment correlation functions of solvent molecules in the interior, surface, and bulk regions for WCA systems. The results are for (a) (10,10) and (b) (12,12) nanotubes. The WCA systems are as defined in the caption of Fig. 3.

Stockmayer molecules inside the (12, 12) tube are comparable with the corresponding bulk values. These findings for this simple non-hydrogen bonded model liquid are in accord with the orientational motion of water inside carbon nanotubes of wide ranges of diameters (3.1 Å–12.6 Å) from (5,5) to (12,12) studied in Ref. 39. Hotta and Sasai[68] also pointed out slower dipole moment relaxation time of water in outer surface of (5,5) nanotube from their molecular dynamics simulations. However, we also note that the reorientational motion of water was reported to be quite fast inside nanotubes than that in the bulk in Ref. 72 where a different flexible model of water was used. Next, we briefly discuss the results of WCA systems which are included in Table III. For these systems, the Stockmayer molecules inside and just outside the repulsive hydrophobic surfaces of nanotubes are perturbed to a greater extent which makes their rotational movement faster. This gives rise to larger values of Θ and smaller values of τ_μ than the bulk values or than the corresponding values for the LJ Systems for (10,10) and (12,12) nanotubes.

V. CONCLUSIONS

In the present work, we have investigated the structure and dynamics of simple dipolar liquids inside and in the outer region of nonpolar nanotubes by means of molecular dynamics simulations. Both solvent and nanotubes are considered at atomistic level. The solvent molecules are modeled by the simple Stockmayer potential while the solute-solvent interaction is modeled through short-range Lennard-Jones and repulsive potentials. Different pore size and solute-solvent interactions are considered in the present study, and a detailed analysis of the solvent density profiles, wetting behavior of the pores, orientational profiles, residence dynamics, and diffusional behavior is made. The current results of the simple dipolar liquid in nanotube systems are compared with those of water in carbon nanotubes reported in earlier studies, although the present model does not include any hydrogen bonding interactions which are believed to be the crucial in determining the solvation behavior of aqueous systems. The present structural and dynamical results assert the generic aspects of many of the structural and dynamical properties of dipolar liquids in hollow hydrophobic pores, especially with respect to trends with changes in pore diameter and solute-solvent interactions.

ACKNOWLEDGMENTS

We thank Department of Science and Technology (DST) for financial support and the University Grants Commission (UGC) for a research fellowship to M. K. Rana during his Ph.D. Part of the calculations was done using the High Performance Computing (HPC) Facility at the Computer Centre, IIT Kanpur.

[1]W. Kauzmann, Adv. Protein Chem. **14**, 1 (1959).
[2]C. Tanford, *The Hydrophobic Effect: Formation of Micelles and Biological Membranes* (Wiley, New York, 1973).
[3]C. Tanford, Science **200**, 1012 (1978).
[4]U.-J. Choe, V. Z. Sun, J.-K. Y. Tan, and D. T. Kamei, *Peptide-Based Materials*, Topics in Current Chemistry (Springer, 2012), Vol. 310, p. 117.
[5]L. Maibaum, A. R. Dinner, and D. Chandler, J. Phys. Chem. B **108**, 6778 (2004).
[6]N. Galamba, J. Phys. Chem. B **117**, 2153 (2013).
[7]R. C. Remsing and J. D. Weeks, J. Phys. Chem. B **117**, 15479 (2013).
[8]G. Jeanmairet, M. Levesque, and D. Borgis, J. Chem. Phys. **139**, 154101 (2013).
[9]W. D. Sasikala and A. Mukherjee, J. Phys. Chem. B **118**, 10553 (2014).
[10]D. M. Huang and D. Chandler, Proc. Natl. Acad. Sci. U. S. A. **97**, 8324 (2000).
[11]K. Leung, A. Luzar, and D. Bratko, Phys. Rev. Lett. **90**, 65502 (2003).
[12]F. H. Stillinger, J. Solution Chem. **2**, 141 (1973).
[13]N. Choudhury and B. M. Pettitt, J. Phys. Chem. B **110**, 8459–8463 (2006).
[14]H. Ashbaugh and L. Pratt, Rev. Mod. Phys. **78**, 159 (2006).
[15]A. Chaimovich and M. S. Shell, Phys. Rev. E **88**, 052313 (2013).
[16]J. G. Davis, K. P. Gierszal, P. Wang, and D. Ben-Amotz, Nature **491**, 582 (2012).
[17]K. Lum, D. Chandler, and J. D. Weeks, J. Phys. Chem. B **103**, 4570 (1999).
[18]Y. Cheng and P. J. Rossky, Nature **392**, 696 (1998).
[19]I. T. S. Li and G. C. Walker, Proc. Natl. Acad. Sci. U. S. A. **108**, 16527 (2011).
[20]K. Lum and D. Chandler, Int. J. Thermophys. **19**, 845 (1998).
[21]D. Huang and D. Chandler, J. Phys. Chem. B **106**, 2047 (2002).
[22]X. Huang, C. J. Margulis, and B. J. Berne, Proc. Natl. Acad. Sci. U. S. A. **100**, 11953 (2003).
[23]R. Zangi, J. Phys. Chem. B **115**, 2303 (2011).
[24]P. R. Pandey and S. Roy, J. Phys. Chem. Lett. **4**, 3692 (2013).

[25]S. Rajamani, T. M. Truskett, and S. Garde, Proc. Natl. Acad. Sci. U. S. A. **102**, 9475 (2005).
[26]P. Liu, X. Huang, R. Zhou, and B. J. Berne, Nature **437**, 159 (2005).
[27]F. Bresme and A. Wynveen, J. Chem. Phys. **126**, 044501 (2007).
[28]L. Hua, R. Zangi, and B. J. Berne, J. Phys. Chem. C **113**, 5244 (2009).
[29]C. Y. Won and N. R. Aluru, J. Am. Chem. Soc. **129**, 2748 (2007).
[30]A. R. Bizzarri and S. Cannistraro, Phys. Rev. E **53**, 3040 (1996).
[31]A. R. Bizzarri and S. Cannistraro, J. Phys. Chem. B **106**, 6617 (2002).
[32]E. Chiavazzo, M. Fasano, P. Asinari, and P. Decuzzi, Nat. Commun. **5**, 4565 (2014).
[33]N. Choudhury, Chem. Phys. **421**, 68 (2013).
[34]N. Choudhury, J. Chem. Phys. **133**, 154515 (2010).
[35]G. Hummer, J. R. Rasaiah, and J. P. Noworyta, Nature **414**, 188 (2001).
[36]K. Koga, G. T. Gao, H. Tanaka, and X. C. Zeng, Nature **412**, 802 (2001).
[37]K. Koga, G. T. Gao, H. Tanaka, and X. C. Zeng, Phys. A **314**, 462 (2002).
[38]W. H. Noon, K. D. Ausman, R. E. Smalley, and J. P. Ma, Chem. Phys. Lett. **355**, 445 (2002).
[39]R. J. Mashl, S. Joseph, N. R. Aluru, and E. Jakobsson, Nano Lett. **3**, 589 (2003).
[40]A. I. Kolesnikov, J. M. Zanotti, C. K. Loong, P. Thiyagarajan, A. P. Moravsky, R. O. Loutfy, and C. J. Burnham, Phys. Rev. Lett. **93**, 035503 (2004).
[41]J. Wang, Y. Zhu, J. Zhou, and X. H. Lu, Phys. Chem. Chem. Phys. **6**, 829 (2004).
[42]A. Striolo, A. A. Chialvo, K. E. Gubbins, and P. T. Cummings, J. Chem. Phys. **122**, 234712 (2005).
[43]Y. C. Liu, Q. Wang, L. Zhang, and T. Wu, Langmuir **21**, 12025 (2005).
[44]Y. C. Liu, Q. Wang, T. Wu, and L. Zhang, J. Chem. Phys. **123**, 234701 (2005).
[45]N. R. de Souza, A. I. Kolesnikov, C. J. Burnham, and C.-K. Loong, J. Phys.: Condens. Matter **18**, S2321 (2006).
[46]A. I. Kolesnikov, C. K. Loong, N. R. de Souza, C. J. Burnham, and A. P. Moravsky, Phys. B: Condens. Matter **385**, 272 (2006).
[47]D. Takaiwa, K. Koga, and H. Tanaka, Mol. Simul. **33**, 127 (2007).
[48]A. Waghe, J. C. Rasaiah, and G. Hummer, J. Chem. Phys. **117**, 10789 (2002).
[49]K. Lee and S. B. Sinnott, Nano Lett. **5**, 793 (2005).
[50]A. Striolo, Nano Lett. **6**, 633 (2006).
[51]B. Mukherjee, P. K. Maiti, C. Dasgupta, and A. K. Sood, J. Chem. Phys. **126**, 124704 (2007).
[52]M. C. Gordillo and J. Mart, J. Chem. Phys. Lett. **329**, 341 (2000).
[53]T. Werder, J. H. Walther, R. L. Jaffe, T. Halicioglu, F. Noca, and P. Koumoutsakos, Nano Lett. **1**, 697 (2001).
[54]J. Marti and M. C. Gordillo, J. Chem. Phys. **114**, 10486 (2001).
[55]L. Liu and G. N. Patey, J. Chem. Phys. **141**, 18C518 (2014).
[56]S. Paul, T. G. Abi, and S. Taraphder, J. Phys. Chem. **140**, 184511 (2014).
[57]M. F. Harrach and B. Drossel, J. Chem. Phys. **140**, 174501 (2014).
[58]Q. Chen, Q. Wang, Y.-C. Liu, and T. Wu, J. Chem. Phys. **140**, 214507 (2014).
[59]J. D. Weeks, D. Chandler, and H. C. Andersen, Science **220**, 787 (1983).
[60]M. P. Allen and D. J. Tildesley, *Computer Simulation of Liquids* (Oxford University, New York, 1987).
[61]O. Beckstein, P. C. Biggin, and Mark S. P. Sansom, J. Phys. Chem. B **105**, 12902 (2001).
[62]O. Beckstein and M. S. P. Sansom, Proc. Natl. Acad. Sci. U. S. A. **100**, 7063 (2003).
[63]O. Beckstein and M. S. P. Sansom, Phys. Biol. **1**, 42 (2004).
[64]A. Striolo, K. E. Gubbins, A. A. Chialvo, and P. T. Cummings, Mol. Phys. **102**, 243 (2004).
[65]R. M. Lynden-Bell and J. C. Rasaiah, J. Chem. Phys. **105**, 9266 (1996).
[66]T. W. Allen, S. Kuyucak, and S.-H. Chung, J. Chem. Phys. **111**, 7985 (1999).
[67]C. Y. Won, S. Joseph, and N. R. Aluru, J. Chem. Phys. **125**, 114701 (2006).
[68]T. Hotta and M. Sasai, J. Phys. Chem. C **111**, 2861 (2007).
[69]J. H. Walther, R. Jaffe, T. Halicioglu, and P. Koumoutsakos, J. Phys. Chem. B **105**, 9980 (2001).
[70]N. Choudhury and B. M. Pettitt, J. Phys. Chem. B **109**, 6422 (2005).
[71]N. Choudhury, J. Phys. Chem. C **111**, 2565 (2007).
[72]J. Marti, E. Guardia, and M. C. Gordillo, Chem. Phys. Lett. **365**, 536 (2002).